Supporting Information

Secondary Guest–Driven Nucleation of N_2O Clathrate Hydrate in Amorphous Ice Mixture under Ultrahigh Vacuum

Bijesh K. Malla,[1,5‡], Soham Chowdhury[1‡], Samir Kumar Nayak[3], Sofia Sara Baji[4], Teena J Mathew[4], Rabin Rajan J Methikkalam[4], Sharma S. R. K. C. Yamijala[3], Rajnish Kumar[2,5,6*] and Thalappil Pradeep[1,2*]*

[1]DST Unit of Nanoscience (DST UNS) and Thematic Unit of Excellence (TUE), Department of Chemistry, Indian Institute of Technology Madras, Chennai 600036, India,

[2]International Centre for Clean Water, IIT Madras Research Park, Chennai 600113, India

[3]Department of Chemistry, Indian Institute of Technology Madras, Chennai 600036, India

[4]Department of Chemistry, Mar Ivanios College, Thiruvananthapuram, Kerala 695015, India

[5]Department of Chemical Engineering, Indian Institute of Technology Madras, Chennai 600036, India

[6]School of Sustainability, Indian Institute of Technology Madras, Chennai 600036, India

Corresponding authors

***Email:** pradeep@iitm.ac.in, rajnish@iitm.ac.in, yamijala@iitm.ac.in

Instrumentation

All the experiments were conducted in an ultrahigh vacuum chamber described in detail elsewhere.[S1] The vacuum chamber is equipped with reflection absorption infrared spectroscopy (RAIRS), temperature-programmed desorption (TPD) mass spectrometry, secondary ion mass spectrometry (SIMS), low energy ion scattering (LEIS) mass spectrometry, and a VUV deuterium continuum. The base pressure of the chamber was ~5×10^{-10} mbar and it was maintained by seven oil-free turbomolecular pumps backed by two scroll pumps (Pfeiffer vacuum). Vacuum was monitored by a Bayard-Alpert (BA) gauge (PBR 260, Pfeiffer Vacuum) and controlled by a MaxiGauge controller (Pfeiffer, Model TPG 256 A).

A Ru(0001) single crystal surface (1.5 cm diameter and 1 mm thick) was used as the substrate to grow the thin ice films. The substrate was mounted on a copper holder and connected to the cold tip of the closed-cycle He cryostat (Coldedge Technologies). The substrate temperature could be varied by a resistive heater (25 Ω) from 8-1000 K, and measured with a K-type thermocouple and a platinum sensor with a temperature accuracy/uncertainty of 0.5 K. Temperature (ramping) was controlled and monitored with a temperature controller, Lakeshore, Model 336. Before each experiment, the Ru(0001) was heated to 400 K repeatedly to ensure cleanliness. It is worth noting that the substrate has no effect in this study due to the multilayer deposition.

Material and Sample Preparation

Millipore water (H_2O of 18.2 MΩ resistivity) was taken in a vacuum-sealed test tube (with a glass-to-metal seal) and was further purified by several freeze–pump–thaw cycles. N_2O (99.9 %, Chemix), ETO (49.5%, 50 % N_2 gas, Vinayaka gas), DME (99.9%, Sigma-Aldrich) gas were used without further purification. 50 % N_2 in ETO gas is confirmed by residual gas analyzer mass spectrum during deposition. This N_2 sublime completely at 40 K, and TPD confirms that only ETO is present in the experimental temperature window (above 120 K).

Thin films of the N_2O-H_2O mixture were created at 10 K by backfilling the vacuum chamber at a total pressure of ~5×10^{-7} mbar for few minutes. Different ratios of N_2O and H_2O (1:5, 1:10, and 1:20) were prepared at 10 K by keeping the total pressure constant and varying the inlet pressure of N_2O and water vapors accordingly. For quantification purposes, we considered that 1.33×10^{-6} mbar exposure for one second, equated to 1 monolayer (ML), was estimated to contain

approximately 1.1×10^{15} molecules cm^{-2}, assuming the ion gauge sensitivity factor of H_2O and N_2O is ~1.0.[S2,S3] The BA gauge sensitivity factors for DME, ETO, and THF are approximately 3–4. Since ETO was introduced as a 50:50 mixture with N_2, we did not determine the exact ML coverage for ETO, DME, or THF. For ternary systems (ETO@N_2O+H_2O, DME@N_2O+H_2O, and THF@N_2O+H_2O), the total deposition time was fixed at 10 minutes. In these cases, the first component (ETO, DME, or THF) was deposited for 200 seconds at 5×10^{-7} mbar, followed by co-deposition of N_2O and H_2O for 400 seconds, using inlet pressures of 1×10^{-7} mbar for N_2O and 4×10^{-7} mbar for H_2O.

For temperature and time-dependent experiments, the as-prepared thin films at 10 K were annealed at a rate of 2 $K \cdot min^{-1}$ to the set temperatures. After maintaining the ice samples at a particular temperature, they were examined by RAIRS.

Computational Details

We employed the Gaussian 16[S4] suite of programs for all quantum chemical calculations. Initially, the geometries of the individual molecules, N_2O, ETO and three distinct CH cages (5^{12}, $5^{12}6^2$, and $5^{12}6^4$ were optimized using the B3LYP[S5] functional in conjunction with the 6-311++G(d,p)[S6] basis set. Subsequently, ETO and N_2O were encapsulated within the clathrate hydrate cages, and the resulting host-guest complexes were subjected to full geometry optimization and frequency calculations at the same level of theory. The calculated vibrational frequencies were scaled by a factor of 0.9679.[S7] Table S1 (Supporting Information 9) lists the calculated frequencies for N_2O and ETO before and after applying the scaling factor. The absence of imaginary frequencies in all optimized structures confirms that true minima were located on the potential energy surface.

Supporting information 1

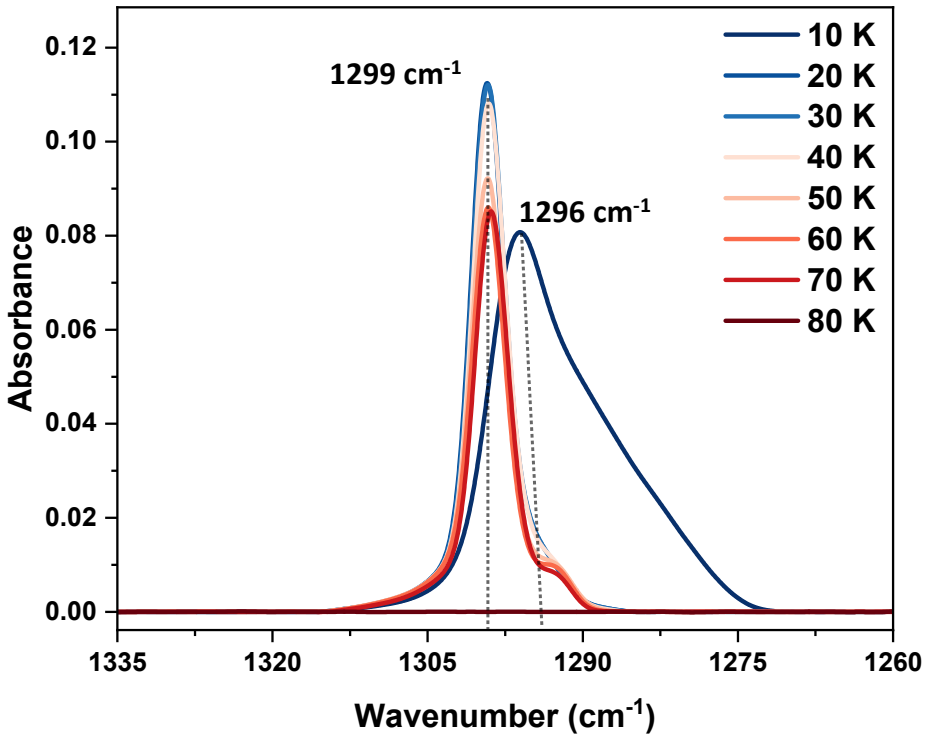

Figure S1. Temperature-dependent RAIR spectra of pure 150 ML N_2O ice in the N–N–O symmetric stretching region.

Supporting information 2

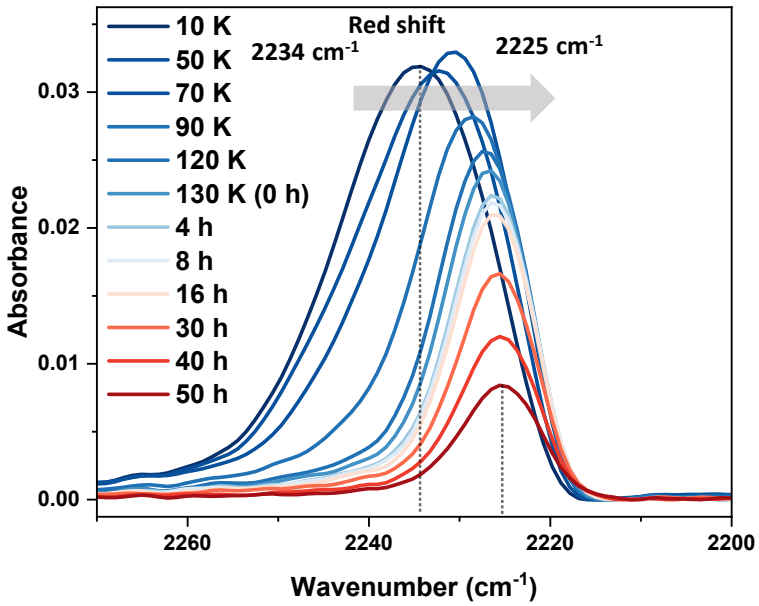

Figure S2. Temperature dependent RAIR spectra of 150 ML of N2O ice in N-N-O asymmetric stretching region.

Supporting information 3

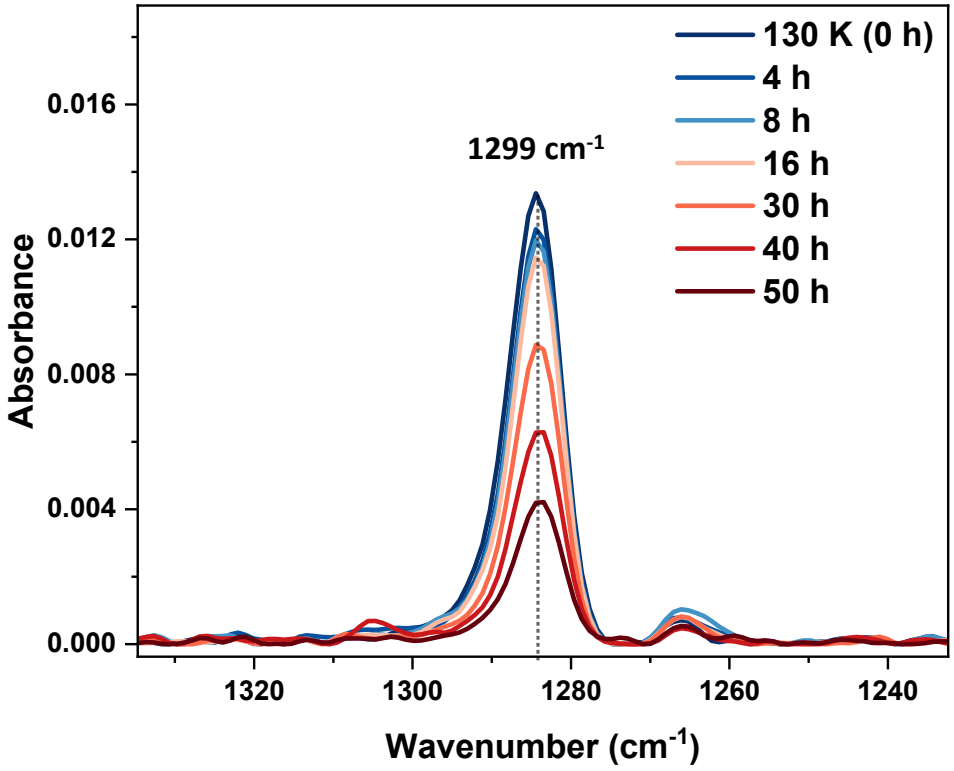

Figure S3. Time-dependent RAIR spectra of a 300 ML N_2O + H_2O ice mixture, showing the N–N–O symmetric stretching region

Supporting information 4

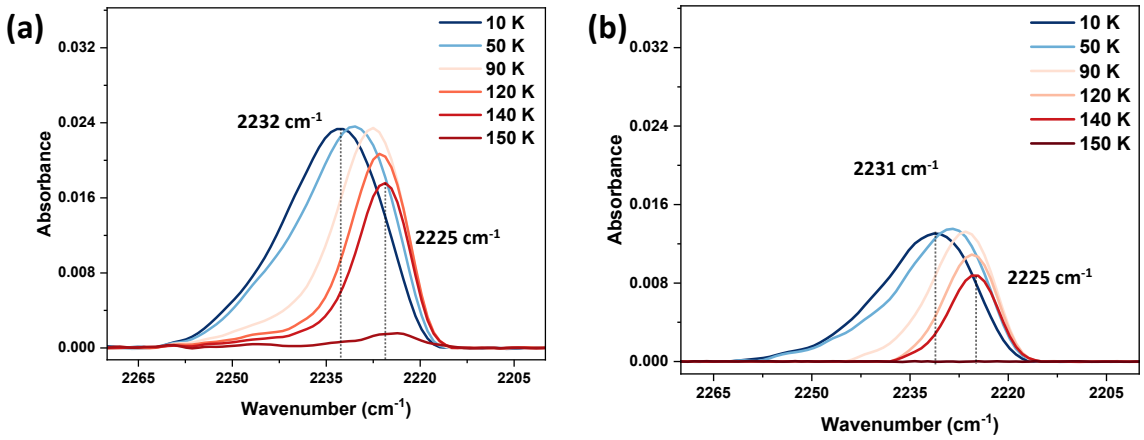

Figure S4. Temperature-dependent RAIR spectra of a 300 ML N_2O + H_2O ice mixture, showing the N–N–O asymmetric stretching region. Figure (a) corresponds to a 1:10 N_2O:H_2O ratio, and figure (b) to a 1:20 ratio.

Supporting information 5

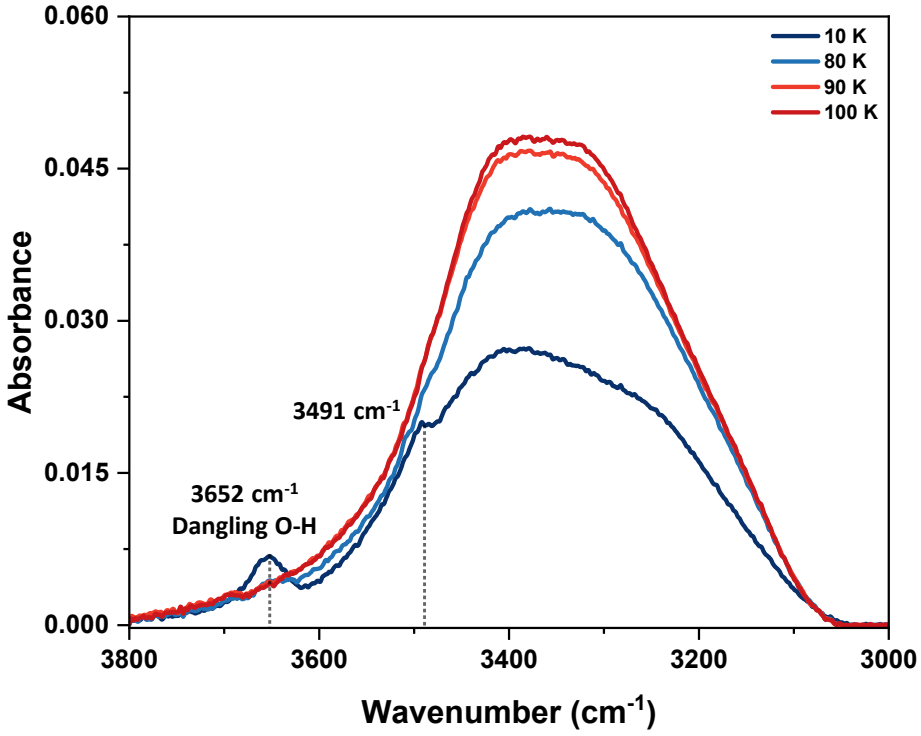

Figure S5. Temperature-dependent RAIR spectra of 300 ML of N_2O-H_2O (1:1) ice mixture in O-H stretching region.

Supporting information 6

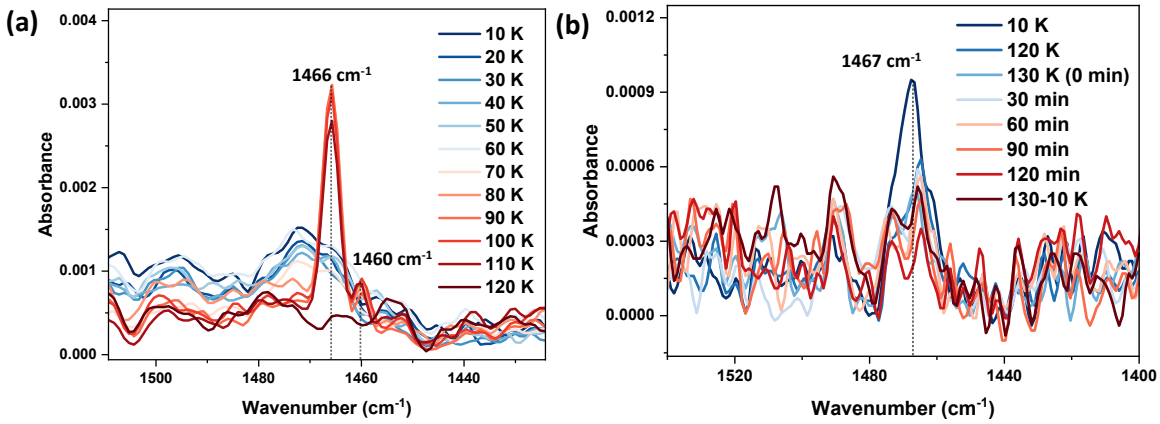

Figure S6. (a) RAIR spectra of pure ETO ice (a) and ETO+H_2O ice mixture (b) in CH_2 bending region.

Supporting information 7

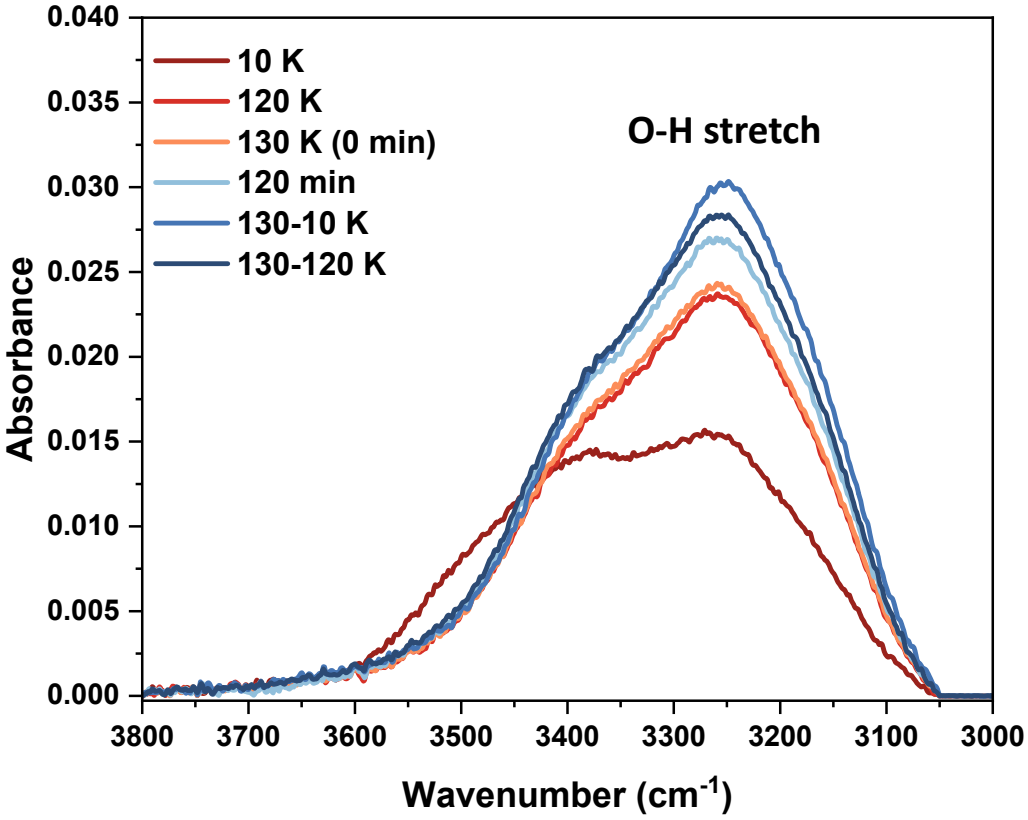

Figure S7. RAIR spectra of ETO + H_2O ice in the O-H stretching region.

Supporting information 8

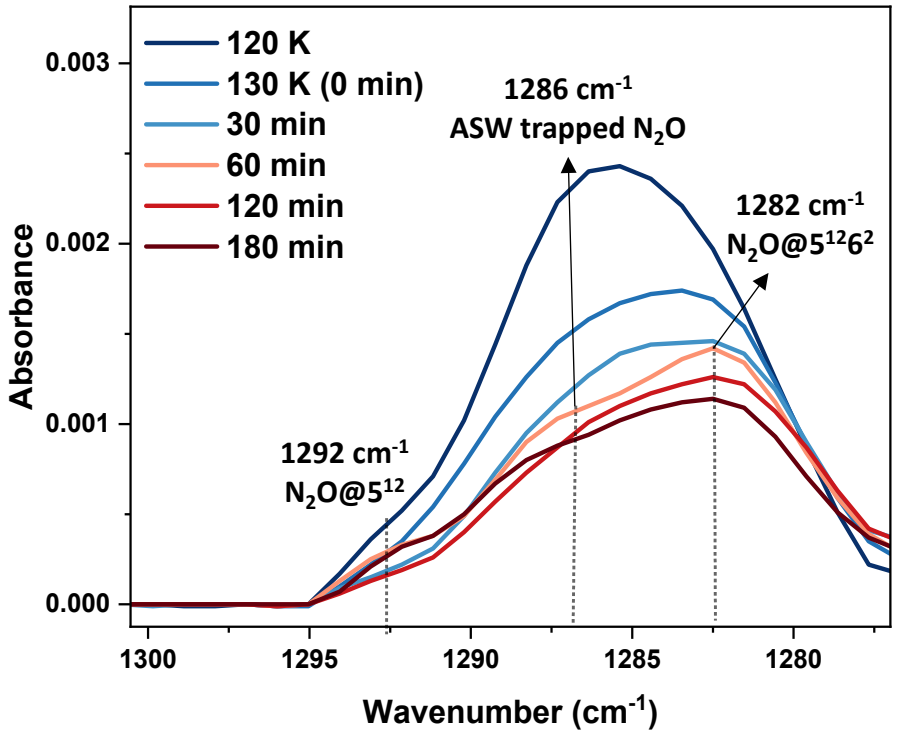

Figure S8. RAIR spectra of ETO@N_2O + H_2O in the N–N–O symmetric stretching region of N_2O.

Supporting information 9

Table S1. Before and after multiplication of scaling factor to calculated frequency.

System	Frequency (Unscaled)	Frequency (Scaled)	System	Frequency (Unscaled)	Frequency (Scaled)
N_2O	2343.15	2267.93	ETO	1298.88	1257.19
$5^{12}@N_2O$	2362.53	2286.69	5^{12}@ETO	1314.38	1272.19
$5^{12}6^2@N_2O$	2348.27	2272.89	$5^{12}6^2$@ETO	1304.58	1262.70
$5^{12}6^4@N_2O$	2345.02	2269.74	$5^{12}6^4$@ETO	1300.93	1259.17

References

(S1) Bag, S.; Bhuin, R. G.; Methikkalam, R. R. J.; Pradeep, T.; Kephart, L.; Walker, J.; Kuchta, K.; Martin, D.; Wei, J. Development of Ultralow Energy (1–10 EV) Ion Scattering Spectrometry Coupled with Reflection Absorption Infrared Spectroscopy and Temperature Programmed Desorption for the Investigation of Molecular Solids. *Rev. Sci. Instrum.* **2014**, *85* (1), 1–7. https://doi.org/10.1063/1.4848895.

(S2) Bartmess, J. E.; Georgiadis, R. M. Empirical Methods for Determination of Ionization Gauge Relative Sensitivities for Different Gases. *Vacuum* **1983**, *33* (3), 149–153. https://doi.org/10.1016/0042-207X(83)90004-0.

(S3) Malla, B. K.; Chowdhury, S.; Paliwal, D.; K. M., H.; Vishwakarma, G.; Methikkalam, R. R. J.; Pradeep, T. Simulated Interstellar Photolysis of N 2 O Ice: Selectivity in Photoproducts. *J. Phys. Chem. C* **2025**, *129* (2), 1120–1128. https://doi.org/10.1021/acs.jpcc.4c06624.

(S4) Gaussian 16, Revision C. 01, M. J. Frisch, G. W. Trucks, H. B. Schlegel, G. E. Scuseria, M. A. Robb, J. R. Cheeseman, G. Scalmani, V. Barone, G. A. Petersson, H. Nakatsuji, X. Li, M. Caricato, A. V. Marenich, J. Bloino, B. G. Janesko, R. Gomperts, B. Mennucci, H. P. Hratchian, J. V. Ortiz, A. F. Izmaylov, J. L. Sonnenberg, D. Williams-Young, F. Ding, F. Lipparini, F. Egidi, J. Goings, B. Peng, A. Petrone, T. Henderson, D. Ranasinghe, V. G. Zakrzewski, J. Gao, N. Rega, G. Zheng, W. Liang, M. Hada, M. Ehara, K. Toyota, R. Fukuda, J. Hasegawa, M. Ishida, T. Nakajima, Y. Honda, O. Kitao, H. Nakai, T. Vreven, K. Throssell, J. A. Montgomery, J. E. Peralta, F. Ogliaro, M. J. Bearpark, J. J. Heyd, E. N. Brothers, K. N. Kudin, V. N. Staroverov, T. A. Keith, R. Kobayashi, J. Normand, K. Raghavachari, A. P. Rendell, J. C. Burant, S. S. Iyengar, J. Tomasi, M. Cossi, J. M. Millam, M. Klene, C. Adamo, R. Cammi, J. W. Ochterski, R. L. Martin, K. Morokuma, O. Farkas, J. B. Foresman, and D. J. Fox, Gaussian, Inc. , Wallingford CT, 2016. Gaussian16.

(S5) Becke, A. D. Density-Functional Thermochemistry. III. The Role of Exact Exchange. J. Chem. Phys. 1993, 98 (7), 5648–5652.

(S6) Krishnan, R.; Binkley, J. S.; Seeger, R.; Pople, J. A. Self-Consistent Molecular Orbital Methods. XX. A Basis Set for Correlated Wave Functions. J. Chem. Phys. 1980, 72 (1), 650–654.

(S7) Andersson, M. P.; Uvdal, P. New Scale Factors for Harmonic Vibrational Frequencies Using the B3LYP Density Functional Method with the Triple-Zeta Basis Set 6-311+G(d,p). J Phys Chem A 2005, 109 (12), 2937–2941.